Chemical Science

EDGE ARTICLE

View Article Online
View Journal | View Issue

Open Access Article. Published on 12 12 2018. Downloaded on 2024/10/07 22:34:38.
This article is licensed under a Creative Commons Attribution-NonCommercial 3.0 Unported Licence.

Check for updates

Cite this: *Chem. Sci.*, 2019, **10**, 1836

All publication charges for this article have been paid for by the Royal Society of Chemistry

Received 16th October 2018
Accepted 6th December 2018

DOI: 10.1039/c8sc04598d

rsc.li/chemical-science

Dynamic polyimine macrobicyclic cryptands – self-sorting with component selection†

Michał Kołodziejski,[abc] Artur R. Stefankiewicz *[bc] and Jean-Marie Lehn *[a]

Self-assembling macrobicyclic cryptand-type organic cages display remarkable self-sorting behavior with efficient component selection. Making use of the dynamic covalent chemistry approach, eight different cages were synthesized by condensation of tris(2-aminopropyl)amine with structurally different dialdehydes. A series of self-sorting experiments were first carried out on simple dynamic covalent libraries. They reveal the influence of different structural features of the aldehyde components on the condensation with two triamine capping units. Subsequently, self-sorting experiments were performed on more complex systems involving several dialdehyde building blocks. Altogether, the results obtained describe the effect of the presence of a heteroatom, of electrostatic interactions, of delocalization and of the flexibility/stiffness of the propensity of a component to undergo formation of a macrobicyclic cage. In the presence of a catalytic amount of acid, the macrobicyclic structure undergoes dynamic component exchange.

Introduction

Since the first synthesis of the macrobicyclic cryptands and cryptates,[1,2] studies on such compounds have been pursued in numerous laboratories and have represented a fascinating area of investigation in supramolecular chemistry.[3,4] The wide interest in macrobicyclic and, by extension, in macropolycyclic entities resides in the rich set of properties (as molecular receptors, catalysts and carriers) enabled by their structural diversity and specific spatial forms, resulting from the use of a variety of building blocks, as well as in their potential uses in areas such as supramolecular engineering and nanotechnology. Much activity has been displayed in the wide area of cage-type compounds and molecular containers.[5–9]

Cryptands have generally been synthesized by stepwise build-up of the macrobicyclic framework based on covalent bond formation.[1–4] In addition, several such structures have later also been obtained by formation of multiple imine bonds.[10–20] The advent and active development of dynamic covalent chemistry (DCC)[21–30] which rests on the implementation of reversible covalent reactions (in particular imine formation) in molecular frameworks, prompts to revisit the area of macrobi(poly)cyclic cryptand-type cage compounds in the light of this approach, which opens up new vistas in synthesis, properties and applications of this class of substances.

Dynamic molecules and materials, molecular as well as supramolecular, have attracted increasing interest in the realm of constitutional dynamic chemistry (CDC)[21,31,32] towards the emergence of adaptive chemistry.[21,32] A particular intriguing feature of such constitutional dynamic systems is the ability to perform component selection in the buildup of their constitution through "self-sorting" processes, introduced initially for the case of "self-recognition" ("homo-self-sorting") in the generation of double and triple stranded helicates.[33] Self-sorting reduces the potential number of combinations of components (thus counteracting entropy) by arranging them into specific organized structures.[34–36] Non-covalent self-sorting in artificial systems, assisted by hydrogen bonds[37] or donor–acceptor interactions[38,39] has been widely explored.[40,41] On the other hand, the initial synthesis and exploration of macrobicyclic cryptand-type molecular cages based on the formation of multiple reversible imine bonds[10,12,15–20] opened the possibility to extend self-sorting processes to the behavior of such dynamic cage architectures. Indeed, the successful high yield generation of these compounds by self-assembly in a single operation based on reversible covalent imine formation, may be considered to involve the operation of "behind-the-scene" dynamic self-sorting. More recently, the chemistry of dynamic covalent cage compounds[42–69] has been subject to inventive developments by several groups based notably on polyimine,[42–60] disulfide[61–65] or orthoester formation.[66–69]

[a]Laboratory of Supramolecular Chemistry, Institut de Science et d'Ingénierie Supramoléculaires (ISIS), UMR 7006, CNRS, Université de Strasbourg, 8 allée Gaspard Monge, 67000 Strasbourg, France. E-mail: lehn@unistra.fr

[b]Faculty of Chemistry, Adam Mickiewicz University, Umultowska 89b, 61-614 Poznań, Poland. E-mail: ars@amu.edu.pl

[c]Center for Advanced Technologies, Adam Mickiewicz University, Umultowska 89c, 61-614 Poznań, Poland

† Electronic supplementary information (ESI) available: Experimental section, characterization of obtained compounds, NMR spectra, CCDC deposition numbers. CCDC 1853998 and 1853999. For ESI and crystallographic data in CIF or other electronic format see DOI: 10.1039/c8sc04598d

This journal is © The Royal Society of Chemistry 2019

Open Access Article. Published on 12 12 2018. Downloaded on 2024/10/07 22:34:38.
This article is licensed under a Creative Commons Attribution-NonCommercial 3.0 Unported Licence.

Dynamic covalent bond formation is thus clearly a means to generate dynamic cage-type compounds (dynamic cryptands) with various differentiated properties and to enable self-sorting in multicomponent libraries. The reversibility of dynamic covalent bonds, such as C=N of imines, enables removal of undesired intermediates ("errors") and leads to the thermodynamically most stable structures. It also provides a pathway to cage-to-cage transformation in solution – a very useful tool that can be used to change the composition of a dynamic library on purpose.[54]

One may thus conclude that organic three-dimensional cage-like architectures can be obtained overall using dynamic covalent bond formation, avoiding complicated, kinetically controlled multistep pathways. Moreover, an important feature of such procedures is the ability to modulate the structural transformations within the component library under the influence of chemical (pH, guest molecule) or physical (temperature, light) stimuli. Such three-dimensional cages suitable for guest inclusion have attracted much attention recently related largely to their use as sensors, drug carriers and catalysts, as well as for storage or isolation of gases.[70,71] However, from the perspective of synthetic self-assembling methodology as well as of functional features, self-sorting protocols add a new dimension to this area and deserve to be closely scrutinized, as they allow for the analysis of the behavior of multicomponent systems.

In the present work, we report the investigation of the effect of structural features of the molecular components on the self-sorting phenomenon in the formation of a variety of imine-based macrobicyclic cryptand-type cage constituents. Moreover, we describe acid-catalysed processes of component exchange between different cages. As a preliminary step, a variety of structurally distinct dialdehydes (**A–H**; Scheme 1) have been reacted with the triamine "tren" (tris(2-aminoethyl)-amine; **T**) to give hexaimine cages, extending the initial work on such processes.[10–16,19] Following the dynamic covalent chemistry approach, dynamic libraries consisting of dialdehydes and triamine components were set up in order to analyse the self-sorting behaviour between the aldehydes employed. In order to be able to evaluate the effects of the structural features of the components, we have restricted the present work to systems involving just the different dialdehydes **A–H** and the triamine **T** in the absence of other agents, such as metal ions.

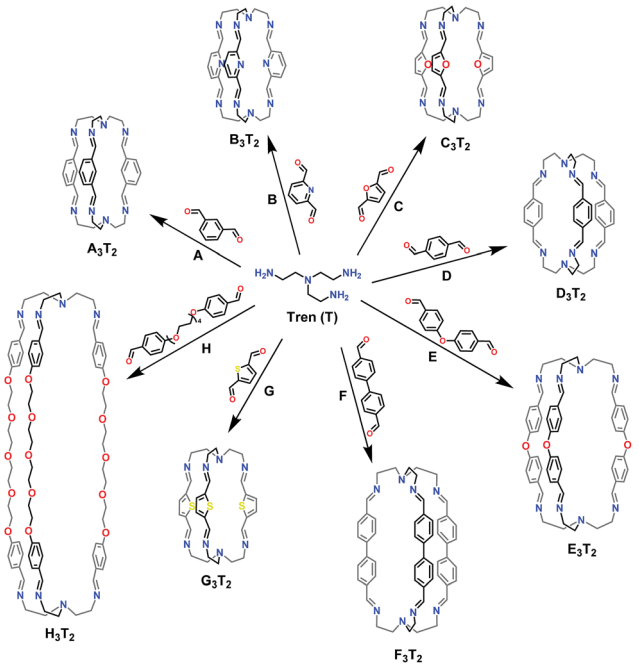

Scheme 1 Molecular structures of dialdehydes (A–H), the triamine (T) and the generated [3 + 2] homoleptic imine-based organic macrobicyclic cryptand cages.

Results and discussion

Synthesis and characterisation of the homoleptic macrobicyclic cages

The reactions examined involved seven aromatic dialdehydes (**A–G**) of fairly similar type and size as well as one (**H**) (very different in both size and flexibility) (Scheme 1). Before performing competitive experiments, the dialdehydes (**A–H**) were separately reacted with triamine **T** in acetonitrile (MeCN) at room temperature. In all cases, substantial precipitates formed within 24 h and were shown subsequently to be the desired cages involving the bridging of two **T** units by three dialdehyde branches by hexa-imine formation, designated as $\mathbf{X_3T_2}$, with **X** = **A–H**. *ortho*-Phthalaldehyde was also included in the initial list of dialdehydes to be tested but it did not react in the same way with **T** as the others and did not provide a cage. All the bulk products gave elemental analyses consistent with the 3 : 2 stoichiometry and all showed ^{1}H NMR spectra (in $CDCl_3$) consistent with the D_3 symmetry expected for the cage where all imine units have the *trans* configuration. The molecular structures of the products also agreed with their ESI-TOF mass spectrometry data. In two cases, $\mathbf{E_3T_2}$ and $\mathbf{F_3T_2}$, details of their solid-state structures were established by single-crystal X-ray crystallography (Fig. 1a and b, respectively). The crystallographic structures of $\mathbf{A_3T_2}$, $\mathbf{B_3T_2}$, $\mathbf{C_3T_2}$ and $\mathbf{D_3T_2}$ cages have been previously described in the literature[16,46–48] as well as those of closely related compounds.[10,15] Thus, crystals of $\mathbf{E_3T_2}\cdot 2CHCl_3$ were obtained as yellow rods by vapour diffusion of diethylether into a chloroform solution. The solid-state molecular structure confirms the structural assignment based on the solution data, showing an extended capsular form with a length of approximately 15 Å, as defined by the distance between the central N atoms of the tren residues, and a twisted chiral shape along this N-to-N axis. The chloroform of crystallisation is not included within the cage, indicating that the lateral dimensions of the cage are unsuited for inclusion, and the lone pairs on the oxygen atoms would appear to be directed out from the cage, indicating that external rather than internal interactions of the cage would be preferred.

Brownish, rod-like crystals of $\mathbf{F_3T_2}$ were obtained by liquid diffusion of diisopropyl ether into a dichloromethane solution at room temperature in a closed vial. The cage unit is again a chiral capsule, though less twisted away from D_{3h} symmetry

Open Access Article. Published on 12 12 2018. Downloaded on 2024/10/07 22:34:38.
This article is licensed under a Creative Commons Attribution-NonCommercial 3.0 Unported Licence.

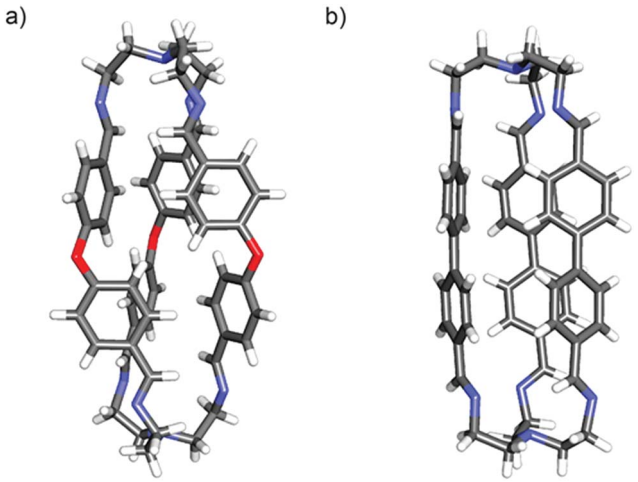

Fig. 1 Solid state X-ray molecular structures of the cages E_3T_2·2$CHCl_3$ (left) and F_3T_2·2$CHCl_3$ (right). Colour code: red, O; blue, N; grey, C; white, H.

than the $\mathbf{E_3T_2}$ cage, and with a separation of the terminal N atoms close to 15 Å. There is no solvent included within the capsule.

Self-sorting experiments

General procedure. After successful synthesis, isolation and characterisation of the eight homoleptic cages $\mathbf{X_3T_2}$ (**X** = **A–H**), we proceeded to the investigation of the self-sorting process in cage formation between triamine **T** with all possible twofold mixtures of the subset **A–E** and **H** of the dialdehydes in chloroform solution from which the cages do not readily precipitate. Note that the products obtained in solution and on precipitation had the same spectroscopic properties. All these self-sorting experiments were conducted under the same conditions (concentration equal to 2×10^{-2} mol dm^{-3}, $CDCl_3$ as a solvent, 1,4-dioxane as an internal standard, 24 h stirring at room temperature, then 24 h stirring at 318.15 K and again 24 h stirring at room temperature to ensure that equilibrium was reached) and the product distribution was conveniently monitored by ^{1}H NMR spectroscopy. The results obtained are summarised in Table 1 (all NMR spectra in ESI, Fig. S9–S23†). Remarkably, the ^{1}H NMR spectra showed that in thirteen of the fifteen simple libraries (*i.e.* two different dialdehydes and the triamine) only a single homoleptic cage was detectable at equilibrium in every case. A mixture of two homoleptic cages was observed in the two systems involving aldehyde pairs **B**/**C** and **D**/**E**.

No formation of heteroleptic systems (mixed-aldehyde components cage species) was observed in any of the tested samples, whether at equilibrium or during its attainment. Thus, the species shown in Scheme 1 suffice to describe the formation behaviour in all systems.

Effect of the presence of a heteroatom on the self-sorting process. In the first self-sorting experiment on the library consisting on **A**, **B** and **T** (3 : 3 : 2 ratio was applied in all experiments) that was carried out, the influence of a heteroaromatic donor atom was investigated. The dialdehyde components **A** and **B** differ only by one atom. The carbon atom in position 2 of isophthalic dicarbaldehyde becomes a nitrogen atom in pyridine-2,6-dicarbaldehyde. Both dialdehydes and their imines contain a fully conjugated system of the aromatic ring and its substituents but only in **B** are attractive interactions possible between the two imine C–H bonds adjacent to the aromatic ring and the adjacent pyridine N atom of another cage arm.[46] A possible additional factor that works in favour of cage $\mathbf{B_3T_2}$ with respect to cage $\mathbf{A_3T_2}$ are intramolecular interactions that may occur between imine C–H bonds and pyridine N lone pair (see ESI, Fig. S29†). Both cages, however, are stabilized through intramolecular hydrogen bonding interactions between the imine C–H bonds of one arm of the cage and the imine N atom of another.[46] These latter interactions are also responsible for the almost identical position of the imine C–H signal in the ^{1}H NMR spectra of both cages. Thus, the heteroaromatic cage $\mathbf{B_3T_2}$ appears to be both kinetically and thermodynamically favoured in this self-sorting experiment and was formed in 92% yield. Cage $\mathbf{A_3T_2}$ is not formed and component **A** remains unreacted in the reaction mixture (Fig. 2). At equilibrium, 8% of unreacted component **B** and triamine **T** are also present.

Effect of the structural flexibility of the components on the self-sorting process. In the self-sorting experiment between components **B**, **H** and **T**, the homoleptic cage $\mathbf{B_3T_2}$ is also preferentially formed in almost quantitative yield (see ESI, Fig. S17†). The second dialdehyde component – **H** – remained unreacted in the mixture. Kinetic factors alone may explain the initially preferred formation of $\mathbf{B_3T_2}$ but it is also the thermodynamically preferred species. An obvious disadvantage of dialdehyde **H** is its flexibility, which must provide an enhanced entropic barrier to both rates and equilibria. Probably more important in explaining the difference in thermodynamic preference for the cage structure (which is but one of many possible cyclic and polymeric imine-containing structures) is the nature of the heteroaromatic unit directly linking the two aldehyde groups of **B**. The lone pair of the N-atom in **B** is suitable for interaction with the imine (and aldehyde) CH atoms,

Table 1 Equilibrium distributions observed for competition experiments between two distinct aldehydes (3 equiv. of each) and amine T (2 equiv.)

T	A	B	C	D	E	H
A		B_3T_2	C_3T_2	A_3T_2	A_3T_2	A_3T_2
B	B_3T_2		B_3T_2 : C_3T_2 56 : 44	B_3T_2	B_3T_2	B_3T_2
C	C_3T_2	B_3T_2 : C_3T_2 56 : 44		C_3T_2	C_3T_2	C_3T_2
D	A_3T_2	B_3T_2	C_3T_2		D_3T_2 : E_3T_2 65 : 35	D_3T_2
E	A_3T_2	B_3T_2	C_3T_2	D_3T_2 : E_3T_2 65 : 35		E_3T_2
H	A_3T_2	B_3T_2	C_3T_2	D_3T_2	E_3T_2	

 This journal is © The Royal Society of Chemistry 2019

Open Access Article. Published on 12 12 2018. Downloaded on 2024/10/07 22:34:38.
This article is licensed under a Creative Commons Attribution-NonCommercial 3.0 Unported Licence.

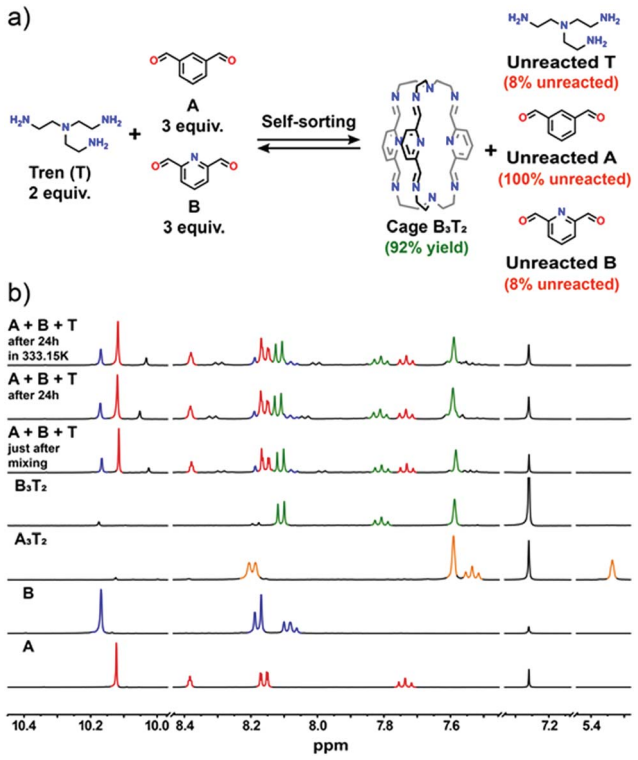

Fig. 2 (a) General scheme of the self-sorting experiment between components A + B + T; (b) comparison of the ^{1}H NMR spectra of all three components recorded over time. The ^{1}H NMR spectra of reaction components and isolated cages are also shown for comparison. Low intensity signals observed in the spectra after component mixing may come from trace amounts of intermediate products such as open chain structures. All NMR spectra were recorded in $CDCl_3$ at 400 MHz.

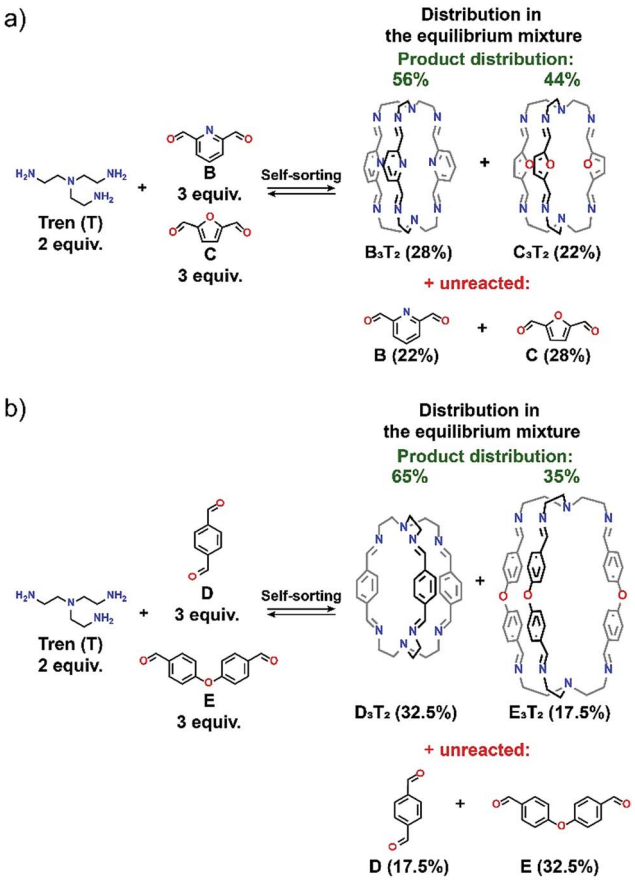

Fig. 3 General schemes presenting product distribution of an equilibrium mixture for libraries consisting of (a) 3B + 3C + 2T and (b) 3D + 3E + 2T.

thus tending to maintain an array better suited to cyclisation than to polymerisation and possibly also providing some activation of the carbonyl centre.

Self-sorting experiments leading to a mixture of two cages. In only two cases (Fig. 3) the competition between two aldehydes for **T** in cage formation was observed. The ^{1}H NMR analysis of the library consisting of **B**, **C** and **T** (see ESI, Fig. S14†) revealed initially the preferential formation of cage $\mathbf{B_3T_2}$ (while at equilibrium both cage species *i.e.* $\mathbf{B_3T_2}$ and $\mathbf{C_3T_2}$ were present in almost equal amounts). Integration of the proton NMR signals provided an equilibrium distribution of 28% of $\mathbf{B_3T_2}$, 22% of $\mathbf{C_3T_2}$, together with unreacted 22% of **B** and 28% of **C** (Fig. 3a). Since both aldehydes contain a heteroaromatic group and form conjugated systems with their substituents, it is unsurprising that there is only a minor difference in their cage formation ability at equilibrium.

In the case of the library comprising component **D**, **E** and **T** a mixture of two cages was again observed, though in this case the formation of $\mathbf{D_3T_2}$ was favoured by about a factor of 2 at equilibrium, the product ratio $\mathbf{D_3T_2} : \mathbf{E_3T_2}$ being 65 : 35 (Fig. 3b). The aldehydes here differ in that the oxygen link in **E** breaks the conjugation of the two halves and introduces a degree of conformational flexibility that is absent in **D** (for NMR spectra see ESI, Fig. S21†).

Self-sorting selectivity in a mixture of six dialdehyde components. The data summarised in Table 1 enable the six aldehydes investigated to be placed in decreasing order of thermodynamic preference in cage formation: **B** = **C** > **A** > **D** > **E** > **H**. To confirm if this order was preserved under conditions where all six aldehydes simultaneously compete for the triamine **T**, we performed a self-sorting experiment on a library consisting of seven components. The sequence of reactions occurring in this system was clearly revealed by following the changes in the ^{1}H NMR spectra covering just the region of the reactant aldehyde CHO proton resonances (Fig. 4). Into a mixture of 3 molar amounts of each of the six dialdehydes (**A**–**E** and **H**), six lots of 2 molar amounts of triamine **T** were titrated progressively. In line with our expectations, after addition of a first dose of **T**, $\mathbf{B_3T_2}$ (with a slight advantage) and $\mathbf{C_3T_2}$ cages began to form almost simultaneously. Addition of another aliquot of **T** led to nearly complete formation of both cages. With the next dose, it was expected to result in the formation of $\mathbf{A_3T_2}$ and indeed it was so, but the ^{1}H NMR spectra showed the simultaneous formation of $\mathbf{D_3T_2}$ in similar amount. The formation of these cages was complete on addition of another dose of **T**. The next stages of this experiment went according to our expectations in that another portion of **T** resulted in formation of $\mathbf{E_3T_2}$ and in the last step $\mathbf{H_3T_2}$ (but here a small excess of triamine was required to complete formation).

Open Access Article. Published on 12 12 2018. Downloaded on 2024/10/07 22:34:38.
This article is licensed under a Creative Commons Attribution-NonCommercial 3.0 Unported Licence.

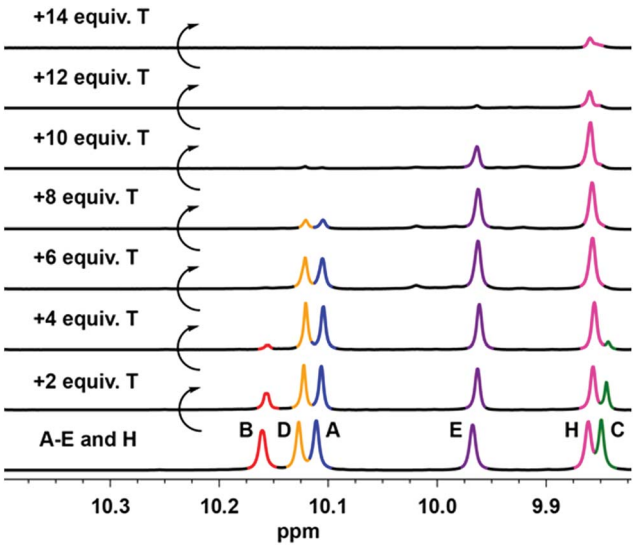

Fig. 4 Changes in aldehyde proton signals of the ^{1}H NMR spectra (400 MHz, $CDCl_3$) during the self-sorting experiment involving titration of 3A + 3B + 3C + 3D + 3E + 3H with appropriate increasing amounts of T. The full spectra of dialdehyde components are shown in ESI.†

This experiment led to the slightly modified order of effectiveness in cage formation of **B** = **C** > **A** = **D** > **E** ≫ **H**. Although it is not clear why the behaviour of **A** and **D** differs slightly in the full mixture from that in the binary one, the observations confirm that the most effective aldehydes of the chosen group are those (**B**, **C**) involving a heteroatom in a simple aromatic unit where there is full conjugation over both imine units. The presence of heteroatoms provides additional possibilities of hydrogen bond formation with the imine C–H, which may further stabilize the cage. Antiparallel orientation of the dipoles of the imine –N= groups and the heteroatoms in the aromatic ring may also be a significant electrostatic factor. Next most effective are the aromatic dialdehydes (**A**, **D**) lacking a heteroatom in the ring but still enabling full conjugation of the imine units with the rings, while least effective are those (**E**, **H**) with some degree of flexibility and an inability to form a conjugated system. Obviously, other factors such as solvation differences may explain some degree of difference but the fact that in all cases it is the cage species that is formed requires that factors controlling the orientation of the imine substituents be considered most important, although here the conformational preferences of the triamine **T** also require consideration.

Effect of the number of aromatic rings and rigidity of the dialdehyde component on the self-sorting process. To explore in greater detail the possible influences of the size of the conjugated unit and the flexibility of the dialdehyde, a further self-sorting titration was conducted with a mixture of just the three dialdehydes **D**, **E** and **F**. The ^{1}H NMR spectra obtained during the titration again clearly showed the sequence of equilibria in the region of the formyl proton resonances (Fig. 5a). Aldehyde **D**, which is capable of forming a fully delocalised diimine unit, reacted the most readily, whereas aldehydes **E** and **F** disappeared more slowly but in a similar manner. As seen in the crystal structure of cage $\mathbf{F_3T_2}$ (see above) the biphenyl unit is significantly twisted, indicating that conjugation/delocalisation over the full diimine unit is decreased and it would be expected to be disrupted by the O-bridge in $\mathbf{E_3T_2}$. Despite the similarity of dialdehydes **E** and **F** in particular, the observations here confirmed once again the absence of any heteroleptic cages.

Effect of the type of heteroatom on the self-sorting process. To get further insights on the effect of the presence of a heteroatom in the dialdehyde components, a titration of a mixture of 3 molar amounts of each of the dialdehydes **B**, **C** and **G** with two-molar doses of **T** was conducted. Changes in the formyl proton ^{1}H NMR signals during the titration are shown in Fig. 5b. Addition of the first portion of triamine **T** initiated the simultaneous formation of $\mathbf{B_3T_2}$ and $\mathbf{C_3T_2}$ in the same ratio as in the original self-sorting experiment **3B** + **3C** + **2T** ($\mathbf{B_3T_2}$: $\mathbf{C_3T_2}$ as 56 : 44). After addition of 4 molar amounts of triamine in total, these two cages were fully formed. With the final dose of **T**, the formation of $\mathbf{G_3T_2}$ was also completed. At this point, there were three homoleptic cages in solution with once again no evidence of the formation of heteroleptic species, despite the similar equilibrium features shown by the dialdehydes **B** and **C**. Given the small advantage of dialdehyde **B** over **C**, the affinity of the dialdehydes for the triamine **T** is: **B** > **C** ≫ **G**. In all three cases, the macrobicyclic cage may be stabilized by H-bonding of the heteroatoms with the imino-CH=N hydrogen. The interaction is expected to follow the sequence N > O > S, which corresponds to the sequence **B** > **C** ≫ **G** observed. In addition, ring size may have an effect when comparing **B** and **C**. Furthermore, the difference between **C** and **G** may result from the stronger H-bonding to O than to S as well as possibly to the smaller size of O (van der Waals radius – 48 ppm for O and 88 ppm for S) and

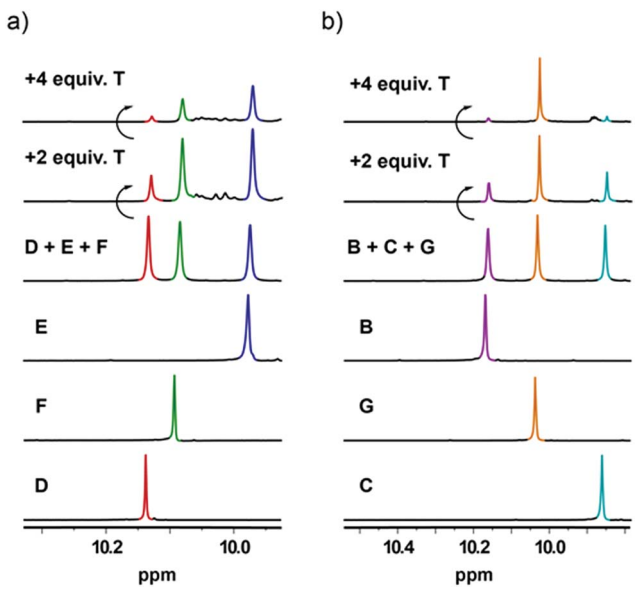

Fig. 5 Comparison of the ^{1}H NMR spectra in the range of the dialdehyde signals for self-sorting experiment on libraries consisting in components (a) 3D + 3E + 3F + 2T and (b) 3B + 3C + 3G + 2T. The aldehyde proton signal of the dialdehyde components are also shown for comparison. All NMR spectra were recorded at 400 MHz in $CDCl_3$ at room temperature.

Open Access Article. Published on 12 12 2018. Downloaded on 2024/10/07 22:34:38.
This article is licensed under a Creative Commons Attribution-NonCommercial 3.0 Unported Licence.

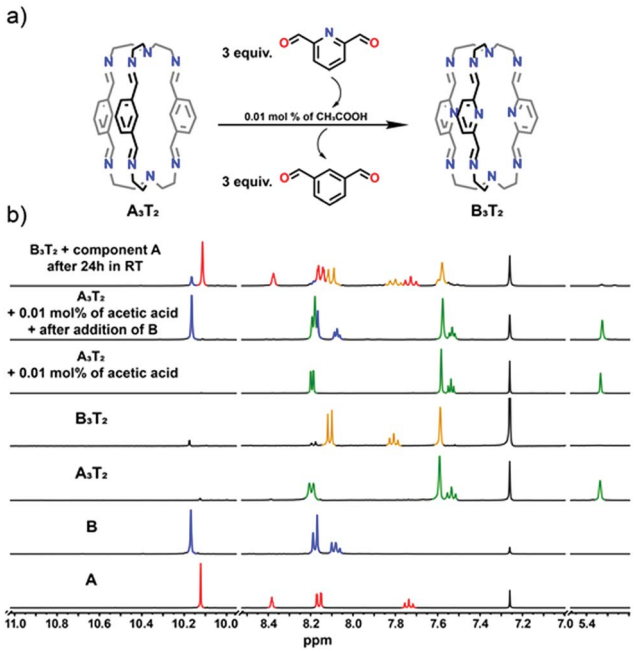

Fig. 6 (a) General scheme of the exchange experiment (A_3T_2 + B → B_3T_2 + A) between components A + B + T; (b) ^{1}H NMR spectra of acid catalysed exchange experiment between cage A_3T_2 and component B. For comparison ^{1}H NMR spectra of components A and B as well as isolated cages A_3T_2 and B_3T_2 are also shown. All NMR spectra were recorded at room temperature in $CDCl_3$.

to the difference in C–O(S) bond lengths (C–O: 0.136 nm; C–S: 0.182 nm). It would indicate that both the smaller radius of the oxygen atom and the shorter C–O bond length are structurally advantageous for cage formation. In addition, the significant difference in the electronegativity between the O and S heteroatoms may favour a more electronegative oxygen atom, enhancing the effect of antiparallel orientation of the dipoles of the imine –CH=N– and of the aromatic heterocyclic groups.

Acid/base assisted equilibration and cage-to-cage transformation. As further confirmation that the observations described above apply to true equilibrium systems, the dynamic nature of the imine bonds under acidic conditions[21] was exploited to examine breakage and reformation (after base addition) of cage mixtures. Using methanesulfonic acid (MSA) and triethylamine (TEA) in sequence, experiments were conducted as outlined for the system **3A** + **3B** + **2T** (see ESI, Fig. S27†).

In the first step, the less preferred cage $\mathbf{A_3T_2}$ was broken into its components by the addition of MSA. The cage was then shown to reform rapidly after the addition of TEA. The dialdehyde **B**, known to form the cage preferentially to **A**, was then added and the ^{1}H NMR spectrum of this mixture showed the absence of any perceptible exchange reaction, *i.e.* the cage $\mathbf{A_3T_2}$ appeared to be stable in the presence of the alternative building block **B**.

Addition of MSA was once again used to dissociate the cage and this final mixture was thereafter made basic with TEA. The only cage species detectable in this solution was then $\mathbf{B_3T_2}$ as expected. Additionally, these results also demonstrate the possibility to perform cage-to-cage mutation.[54]

These experiments established the lability of the cages in acidic media but involved their complete breakage. As an extension, component exchange from ($\mathbf{A_3T_2}$ + **B**) to ($\mathbf{B_3T_2}$ + **A**) was also investigated using a weak acid at catalytic concentrations to see if exchange of components could be observed in the absence of detectable cage dissociation. While reaction of $\mathbf{A_3T_2}$ with **B** under such conditions (0.01 mol% catalyst) proved to be slow, cage breakup was not observed other than in that after 24 h reaction, the cage signals in the ^{1}H NMR spectrum (Fig. 6) were those of $\mathbf{B_3T_2}$ and were accompanied by those of free **A**. Thus, the strong equilibrium preference for formation of the cage involving **B** and not **A** was once more confirmed.

Conclusions

As demonstrated herein, remarkable self-sorting behavior of high selectivity takes place in the formation of imine-based macrobicyclic cryptand-type organic cages from mixtures of different dialdehyde components reacting with the same capping triamine (see also related processes in ref. 42–53). The structure of the components (their electronic properties, flexibility, presence of a heteroatom, *etc.*) plays a decisive role in the selective formation of given polyimine cages out of the different structural variations that may be generated from a mixture of very similar dialdehyde building blocks. Structural exploration supports the conclusion that the presence of a heteroatom in a simple aromatic unit favors the cage formation. The results point to the operation of different structural factors comprising attractive H-bonding interactions and electrostatic effects between the imine groups and heteroatomic centers as well as the generation of a conjugated system. Some degree of flexibility and hindrance to optimization of electronic interactions reduce the effectiveness of a component in the self-sorting process. Furthermore, once formed, a given cage may be kinetically trapped, thus forming an out-of-equilibrium mixture. However, in the presence of an agent capable of breaking the imine bonds in the hexaimine structure, exchange of components becomes possible, as expected from the dynamic covalent chemistry of imines, resulting in the generation of the equilibrium state. Developments towards the kinetic behavior of the self-sorting processes, the generation of kinetically trapped out-of-equilibrium states and the encapsulation of substrate molecules may be envisaged.

Conflicts of interest

There are no conflicts to declare.

Acknowledgements

The authors acknowledge financial support from the ERC (Advanced Research Grant SUPRADAPT 290585), the ANR DYNAFUN grant No. ANR-15-CE29-0009-01 and the University of Strasbourg. Financial support was also provided by the National Science Centre in Poland (MK, grant PRELUDIUM UMO-2017/25/N/ST5/00942) and the National Centre for Research and Development (ARS, grant LIDER/024/391/L-5/13/NCBR/2014).

Open Access Article. Published on 12 12 2018. Downloaded on 2024/10/07 22:34:38.
This article is licensed under a Creative Commons Attribution-NonCommercial 3.0 Unported Licence.

We thank Li-Yuan Huang (Strasbourg, Guangzhou) for related work towards polyimine cage compounds. We also thank Prof. Jack Harrowfield for helpful discussions.

Notes and references

1 B. Dietrich, J. M. Lehn and J. P. Sauvage, *Tetrahedron Lett.*, 1969, **10**, 2885–2888.
2 B. Dietrich, J. M. Lehn, J. P. Sauvage and J. Blanzat, *Tetrahedron*, 1973, **29**, 1629–1645.
3 J. M. Lehn, *Acc. Chem. Res.*, 1978, **11**, 49–57.
4 L. Fabbrizzi, *Cryptands and Cryptates*, World Scientific Publishing Company, 2017.
5 P. Ballester, M. Fujita and J. Rebek, *Chem. Soc. Rev.*, 2015, **44**, 392–393.
6 D. S. Kim and J. L. Sessler, *Chem. Soc. Rev.*, 2015, **44**, 532–546.
7 D. Ajami, L. Liu and J. Rebek Jr, *Chem. Soc. Rev.*, 2015, **44**, 490–499.
8 S. H. A. M. Leenders, R. Gramage-Doria, B. de Bruin and J. N. H. Reek, *Chem. Soc. Rev.*, 2015, **44**, 433–448.
9 G. Markiewicz, A. Jenczak, M. Kołodziejski, J. J. Holstein, J. K. M. Sanders and A. R. Stefankiewicz, *Nat. Commun.*, 2017, **8**, 15109.
10 J. Jazwinski, J.-M. Lehn, D. Lilienbaum, R. Ziessel, J. Guilhem and C. Pascard, *J. Chem. Soc., Chem. Commun.*, 1987, 1691–1694.
11 R. Abidi, F. Arnaud-Neu, M. G. B. Drew, S. Lahely, D. Marrs, J. Nelson and M.-J. Schwing-Weill, *J. Chem. Soc., Perkin Trans. 2*, 1996, 2747–2755.
12 D. MacDowell and J. Nelson, *Tetrahedron Lett.*, 1988, **29**, 385–386.
13 D. J. Marrs, V. McKee, J. Nelson, Q. Lu and C. J. Harding, *Inorg. Chim. Acta*, 1993, **211**, 195–202.
14 Q. Lu, J.-M. Latour, C. J. Harding, N. Martin, D. J. Marrs, V. McKee and J. Nelson, *J. Chem. Soc., Dalton Trans.*, 1994, 1471–1478.
15 J.-M. Lehn, J.-P. Vigneron, I. Bkouche-Waksman, J. Guilhem and C. Pascard, *Helv. Chim. Acta*, 1992, **75**, 1069–1077.
16 D. McDowell, J. Nelson and V. McKee, *Polyhedron*, 1989, **8**, 1143–1145.
17 O. Kocian, R. J. Mortimer and P. D. Beer, *Tetrahedron Lett.*, 1990, **31**, 5069–5072.
18 R. Menif, A. E. Martell, P. J. Squattrito and A. Clearfield, *Inorg. Chem.*, 1990, **29**, 4723–4729.
19 J. de Mendoza, E. Mesa, J.-C. Rodríguez-Ubis, P. Vázquez, F. Vögtle, P.-M. Windscheif, K. Rissanen, J.-M. Lehn, D. Lilienbaum and R. Ziessel, *Angew. Chem., Int. Ed. Engl.*, 1991, **30**, 1331–1333.
20 V. McKee, J. Nelson and R. M. Town, *Chem. Soc. Rev.*, 2003, **32**, 309–325.
21 J.-M. Lehn, *Chem.–Eur. J.*, 1999, **5**, 2455–2463.
22 S. J. Rowan, S. J. Cantrill, G. R. L. Cousins, J. K. M. Sanders and J. F. Stoddart, *Angew. Chem., Int. Ed.*, 2002, **41**, 898–952.
23 P. T. Corbett, J. Leclaire, L. Vial, K. R. West, J.-L. Wietor, J. K. M. Sanders and S. Otto, *Chem. Rev.*, 2006, **106**, 3652–3711.
24 S. Ladame, *Org. Biomol. Chem.*, 2008, **6**, 219–226.
25 S. O. J. N. H. Reek, *Dynamic Combinatorial Chemistry*, Wiley-VCH, Weinheim, 2010.
26 B. L. Miller, *Dynamic Combinatorial Chemistry*, Wiley, Chichester, 2010.
27 M. E. Belowich and J. F. Stoddart, *Chem. Soc. Rev.*, 2012, **41**, 2003–2024.
28 Y. Jin, C. Yu, R. J. Denman and W. Zhang, *Chem. Soc. Rev.*, 2013, **42**, 6634–6654.
29 S. P. Black, J. K. M. Sanders and A. R. Stefankiewicz, *Chem. Soc. Rev.*, 2014, **43**, 1861–1872.
30 *Dynamic Covalent Chemistry: Principles, Reactions, and Applications*, ed. W. Zhang and J. Yinghua, Wiley-VCH, Weinheim, 2018.
31 J.-M. Lehn, in *Constitutional Dynamic Chemistry*, ed. M. Barboiu, Springer Berlin Heidelberg, Berlin, Heidelberg, 2012, pp. 1–32.
32 J.-M. Lehn, *Chem. Soc. Rev.*, 2007, **36**, 151–160.
33 R. Kramer, J. M. Lehn and A. Marquis-Rigault, *Proc. Natl. Acad. Sci. U. S. A.*, 1993, **90**, 5394–5398.
34 M. M. Safont-Sempere, G. Fernández and F. Würthner, *Chem. Rev.*, 2011, **111**, 5784–5814.
35 K. Osowska and O. Š. Miljanić, *Synlett*, 2011, **2011**, 1643–1648.
36 Z. He, W. Jiang and C. A. Schalley, *Chem. Soc. Rev.*, 2015, **44**, 779–789.
37 A. S. Singh and S.-S. Sun, *Chem. Commun.*, 2012, **48**, 7392–7394.
38 K. Mahata, M. L. Saha and M. Schmittel, *J. Am. Chem. Soc.*, 2010, **132**, 15933–15935.
39 W. Drożdż, M. Kołodziejski, G. Markiewicz, A. Jenczak and A. Stefankiewicz, *Int. J. Mol. Sci.*, 2015, **16**, 16300.
40 M. A. Squillaci, G. Markiewicz, A. Walczak, A. Ciesielski, A. R. Stefankiewicz and P. Samorì, *Chem. Commun.*, 2017, **53**, 9713–9716.
41 K. Tahara, T. Fujita, M. Sonoda, M. Shiro and Y. Tobe, *J. Am. Chem. Soc.*, 2008, **130**, 14339–14345.
42 T. Jiao, G. Wu, L. Chen, C.-Y. Wang and H. Li, *J. Org. Chem.*, 2018, **83**, 12404–12410.
43 G. Zhu, Y. Liu, L. Flores, Z. R. Lee, C. W. Jones, D. A. Dixon, D. S. Sholl and R. P. Lively, *Chem. Mater.*, 2018, **30**, 262–272.
44 T. Mitra, K. E. Jelfs, M. Schmidtmann, A. Ahmed, S. Y. Chong, D. J. Adams and A. I. Cooper, *Nat. Chem.*, 2013, **5**, 276.
45 K. Ono and N. Iwasawa, *Chem.–Eur. J.*, 2018, **24**, 1–14.
46 M. G. B. Drew, V. Felix, V. McKee, G. Morgan and J. Nelson, *Supramol. Chem.*, 1995, **5**, 281–287.
47 M. G. B. Drew, D. Marrs, J. Hunter and J. Nelson, *J. Chem. Soc., Dalton Trans.*, 1992, 11–18.
48 V. McKee, W. T. Robinson, D. McDowell and J. Nelson, *Tetrahedron Lett.*, 1989, **30**, 7453–7456.
49 N. Giri, C. E. Davidson, G. Melaugh, M. G. Del Pópolo, J. T. A. Jones, T. Hasell, A. I. Cooper, P. N. Horton, M. B. Hursthouse and S. L. James, *Chem. Sci.*, 2012, **3**, 2153–2157.
50 G. Zhang and M. Mastalerz, *Chem. Soc. Rev.*, 2014, **43**, 1934–1947.

 This journal is © The Royal Society of Chemistry 2019

Open Access Article. Published on 12 12 2018. Downloaded on 2024/10/07 22:34:38.
This article is licensed under a Creative Commons Attribution-NonCommercial 3.0 Unported Licence.

51 P. Kieryk, J. Janczak, J. Panek, M. Miklitz and J. Lisowski, *Org. Lett.*, 2016, **18**, 12–15.
52 X.-Y. Hu, W.-S. Zhang, F. Rominger, I. Wacker, R. R. Schroder and M. Mastalerz, *Chem. Commun.*, 2017, **53**, 8616–8619.
53 J. C. Lauer, W.-S. Zhang, F. Rominger, R. R. Schröder and M. Mastalerz, *Chem.–Eur. J.*, 2018, **24**, 1816–1820.
54 K. Acharyya, S. Mukherjee and P. S. Mukherjee, *J. Am. Chem. Soc.*, 2013, **135**, 554–557.
55 K. Acharyya and P. S. Mukherjee, *Chem.–Eur. J.*, 2014, **20**, 1646–1657.
56 P. Skowronek, B. Warzajtis, U. Rychlewska and J. Gawronski, *Chem. Commun.*, 2013, **49**, 2524–2526.
57 P. Skowronek and J. Gawronski, *Org. Lett.*, 2008, **10**, 4755–4758.
58 D. Beaudoin, F. Rominger and M. Mastalerz, *Angew. Chem., Int. Ed.*, 2017, **56**, 1244–1248.
59 C. J. Pugh, V. Santolini, R. L. Greenaway, M. A. Little, M. E. Briggs, K. E. Jelfs and A. I. Cooper, *Cryst. Growth Des.*, 2018, **18**, 2759–2764.
60 T. Hasell, X. Wu, J. T. A. Jones, J. Bacsa, A. Steiner, T. Mitra, A. Trewin, D. J. Adams and A. I. Cooper, *Nat. Chem.*, 2010, **2**, 750–755.
61 D. Xu and R. Warmuth, *J. Am. Chem. Soc.*, 2008, **130**, 7520–7521.
62 N. Christinat, R. Scopelliti and K. Severin, *Angew. Chem., Int. Ed.*, 2008, **47**, 1848–1852.
63 A. R. Stefankiewicz, M. R. Sambrook and J. K. M. Sanders, *Chem. Sci.*, 2012, **3**, 2326–2329.
64 W. Drożdż, C. Bouillon, C. Kotras, S. Richeter, M. Barboiu, S. Clément, A. R. Stefankiewicz and S. Ulrich, *Chem.–Eur. J.*, 2017, **23**, 18010–18018.
65 A. R. Stefankiewicz and J. K. M. Sanders, *Chem. Commun.*, 2013, **49**, 5820–5822.
66 M. von Delius, *Synlett*, 2016, **27**, 177–180.
67 R.-C. Brachvogel, F. Hampel and M. von Delius, *Nat. Commun.*, 2015, **6**, 7129.
68 R.-C. Brachvogel and M. von Delius, *Chem. Sci.*, 2015, **6**, 1399–1403.
69 R.-C. Brachvogel, H. Maid and M. von Delius, *Int. J. Mol. Sci.*, 2015, **16**, 20641.
70 M. W. Schneider, H.-J. Siegfried Hauswald, R. Stoll and M. Mastalerz, *Chem. Commun.*, 2012, **48**, 9861–9863.
71 A. Galan and P. Ballester, *Chem. Soc. Rev.*, 2016, **45**, 1720–1737.